

RSC Advances



This is an *Accepted Manuscript*, which has been through the Royal Society of Chemistry peer review process and has been accepted for publication.

Accepted Manuscripts are published online shortly after acceptance, before technical editing, formatting and proof reading. Using this free service, authors can make their results available to the community, in citable form, before we publish the edited article. This *Accepted Manuscript* will be replaced by the edited, formatted and paginated article as soon as this is available.

You can find more information about *Accepted Manuscripts* in the [Information for Authors](#).

Please note that technical editing may introduce minor changes to the text and/or graphics, which may alter content. The journal's standard [Terms & Conditions](#) and the [Ethical guidelines](#) still apply. In no event shall the Royal Society of Chemistry be held responsible for any errors or omissions in this *Accepted Manuscript* or any consequences arising from the use of any information it contains.

Theoretical Analysis of the U L₃-Edge NEXAFS in U Oxides

Connie J. Nelin

Consultant, Austin, TX 78730, USA

Paul S. Bagus*

Department of Chemistry, University of North Texas, Denton, TX 76203-5017, USA

Eugene S. Ilton

Pacific Northwest National Laboratory, Richland, WA 99352, USA

Abstract: Rigorous theoretical studies of the electronic structure to describe the Uranium L₃ near edge X-ray absorption fine structure, NEXAFS, of different oxidation states of U in UO_x are reported. Key features of the spectra are related to the ligand field splitting of the excited state orbitals. Furthermore, the ligand field splitting is related to the different extent of covalent mixing that occur at different U-O distances for the different oxidation states. The theoretical relative energies and intensities are based on electronic wavefunctions for cluster models of the oxides. This allows a direct relationship to be established between the L₃-edge NEXAFS features and the covalent mixing in the oxides. Correlations are established between the width of the L₃ NEXAFS and the U-O distance and these correlations are shown to reflect the character of the chemical interaction between the U cations and the O anions.

Ab initio theoretical studies of the Uranium L₃ near edge X-ray adsorption fine structure, NEXAFS, of different oxidation states of U in UO_x are reported. These studies show the origin of the shape and the width of the NEXAFS peak and show how these features can be used to identify the U oxidation state. NEXAFS, also described by the acronym XANES for X-ray adsorption near edge structure, can provide information about the electronic structure of the material, especially with respect to the frontier orbital open or unoccupied levels. [1] An early paper by Kalkowski *et al.* [2] on the NEXAFS of uranium compounds examined several edges from L₃ to O_{4,5}. Many subsequent papers have reported the NEXAFS of different U phases and U-bearing compounds, for example Refs. [3-6]. But, very few papers have focused on the theoretical interpretation of the NEXAFS of uranium; moreover, those that have are often based on the use of Anderson model Hamiltonians. [7-9] However, this approach does not explicitly include the covalent mixing of cation and ligand orbitals in the electronic structure of the materials. [10, 11] Further, it is common, with this model, to adjust parameters to fit core-level spectra; see, for example, Refs. [10, 12, 13]. Theoretical studies of U-oxide NEXAFS [4] have also been based on

the real space multiple scattering, RSMS, approach implemented in the FEFF program, [14] which, however, does not directly treat the multiplet coupling of the open shell electrons. With both the Anderson model Hamiltonians [7-9] and the RSMS methods, [14] it is not straightforward to relate the calculated XAS to chemistry and chemical bonding. For example, although the FEFF results for the U L₃-edge NEXAFS of several uranium ternary oxides presented in Ref. [4] are in reasonable agreement with experiment, there is no discussion of ligand field splitting or of covalent mixing of O(2p) and U frontier orbitals. This is in strong contrast to our approach where we focus on establishing direct connections between the NEXAFS and the chemical interactions in U oxides. This chemistry is represented by the fundamental concepts of covalent mixing and the ligand field splitting in the octahedral symmetry of the oxides considered. Our theoretical approach for the U L₃-edge NEXAFS is based on the determination of fully relativistic wavefunctions, WF's, where the angular momentum coupling, or multiplets, of the open shell electrons is rigorously treated and where parameters are not adjusted to fit experiment. Furthermore, covalency is naturally incorporated into our model. Thus, our methods allow us to relate individual NEXAFS transitions to the electronic structure and covalent mixing in the oxides and to draw connections between features of the NEXAFS and the chemistry and physics of the oxides.

Here, we focus on the L₃ NEXAFS of U(VI), U(V), and U(IV) in octahedral uranate coordination, where uranate refers to a symmetric bonding environment that lacks the short trans-dioxo bonds that typify uranyl coordination. Our rigorous theoretical analysis shows that the L₃-edge NEXAFS distinguish U(V) from U(VI), when both are in octahedral uranate coordination, as suggested in prior experimental work. In particular, this work appears to show that the white line peak is broader nearer the top for U(VI) compared to U(V). [4-6] More importantly, we use our rigorous *ab initio* approach in order to understand why the L₃ NEXAFS of U in octahedral coordination differ between different oxidation states. We also test and validate our theoretical methods for the NEXAFS of fluorite U(IV) in UO₂.

The materials models are embedded UO₆ clusters with appropriate U-O bond distances, designated d(U-O) [10, 12]. For U(VI), d(U-O)=2.09Å, which corresponds to δ-UO₃; [15] for U(V), we use a structure with d(U-O)=2.15Å; [16] and for U(IV), we use an idealized octahedral structure with an average

$d(\text{U-O})=2.22 \text{ \AA}$. [4] For U(VI) and U(V), we consider variations of the lattice constants about the $d(\text{U-O})$ values listed above. These variations of $d(\text{U-O})$ allow us to establish a direct link between the features of the NEXAFS and the changes in the covalent chemical interaction between U and the O ligands. [10, 12] For U(IV), we also determined the L_3 NEXAFS for the fluorite structure of UO_2 using an embedded UO_8 cluster with $d(\text{U-O})=2.37 \text{ \AA}$. [12, 17] The ground state configuration for U(VI) UO_6 is closed shell, while the ground state configurations for U(V) and U(IV) UO_6 have 1 or 2 electrons, respectively, in a shell of the 14 nearly degenerate spinors that, in the limit of an isolated cation, are U(5f) spinors. Orbitals, four-component spinors, are optimized separately for ground and core-hole configurations and substantial covalent mixing is found between the cation frontier f and d orbitals and the O(2p) orbitals. [10, 11] In the present paper, we use the sizes of the excited orbitals obtained from our fully relativistic variational procedure as a unique measure of the relative extents of the covalent mixing in different orbitals. These sizes clearly demonstrate it is not proper to regard the orbitals of the system as either pure cation or pure anion orbitals. The WF's constructed from these optimized orbitals are mixtures of configurations, described as configuration mixing, CI, WF's, [10, 18] where the determinants that are mixed are formed by distributing the open shell electrons over an active space of orbitals. This CI treatment accurately describes the orbital and spin angular momentum coupling taking account of the spin-orbit interaction. [19] It is able to describe, on an equal footing, ligand field and spin-orbit splittings; [17, 19] there is no need to include an adjustable parameter as in DFT+U treatments. [20] The active orbital space for excitations from the $2p_{3/2}$ shell includes low lying spinors with gerade, g, symmetry; only g symmetry is considered for these excitations since they are the only dipole allowed excitations from the ungerade $2p_{3/2}$ spinors. These low lying spinors can be grouped into sets of spin-orbit and ligand field split orbitals. Following common usage, [2, 4, 5] we label these orbitals with the notation for shells in the isolated U cation as 6d, 7s, and 7d. The assignment is based on the size of the orbitals as measured by $r_{\text{avg}} = [\langle r^2 \rangle]^{1/2}$ with 6d being smaller than 7d. The 6d, 7s, and 7d orbitals belong to the a_{1g} , e_g , and t_{2g} cubic symmetries where the t_{2g} orbitals are further spin-orbit split. [21] While the notations a_{1g} , e_g , and t_{2g} , are not strictly valid once spin-orbit splitting is taken into account, they are good approximations for these orbitals,

where, as we shall see, the spin-orbit splitting is small. We determine relative intensities, I_{rel} , of the NEXAFS transitions from dipole transition matrix elements. Details of the calculations are given in the ESI.

The theoretical predictions of the NEXAFS for the octahedral UO_6 cluster models of U(VI), U(V), and U(IV) are plotted in Figs. 1(a-c). The directly calculated dipole I_{rel} are broadened with a Voigt convolution of a Lorentzian of 7.5 eV FWHM to account for the lifetime of the $2p_{3/2}$ hole [22] and a Gaussian of 3.0 eV FWHM to account for experimental resolution in the NEXAFS measurements. Individual contributions are shown under the envelope of the full intensity summed over all final states. The relative energy is set so that the inflection point of the leading edge of the curve is at $E_{\text{rel}}=0$ eV. We first consider the NEXAFS for U(VI), Fig. 1(a), because the open shell structure is simpler than for U(V) and U(IV) making it is possible to examine contributions to the spectrum in detail. For an excitation of one of the 4 U($2p_{3/2}$) electrons into one of the 10 unoccupied spinors labeled as 6d, there are 40 possible determinants. In the space of these 40 determinants, the states that are solutions of the CI Hamiltonian are distributed over 17 groups, referred to as terms, where the members of a group are degenerate in energy. Most of the 17 terms have zero intensity by symmetry; from Fig. 1(a), the main intensity comes from three terms. The most intense peak, at $E_{\text{rel}}=8.8$ eV, is dominated by configurations with one electron in the e_g shell. The peaks at $E_{\text{rel}}=2.6$ and 2.1 eV are dominated by one electron in one of the spin-orbit split t_{2g} shells. The relative intensities, or branching ratios, of these peaks do not follow from the degeneracies of the shells. If they had, the peak at $E_{\text{rel}}=2.1$ eV would have been of comparable intensity to that at $E_{\text{rel}}=8.8$ eV, since the e_g and the lowest spin-orbit split t_{2g} shells are both 4 fold degenerate; instead the peak at $E_{\text{rel}}=2.1$ eV is less intense by a factor of 2. The branching ratios follow from the details of the angular momentum coupling of the $2p_{3/2}$ and 6d shells. [23, 24] In the non-relativistic limit, dipole transitions from the initial $^1A_{1g}$ term are allowed only to the $^1T_{1u}$ term of $2p^56d^1$; however, once spin-orbit coupling is taken into account, this allowed Russell-Saunders multiplet is distributed over several allowed terms. [24] While a detailed analysis of the branching ratios is beyond the scope of this paper, we will show below how changes in the branching ratio may affect the shape of the L_3 NEXAFS peaks. Thus, the branching ratios,

which depend, in part, on the U-O distance, potentially provide another fingerprint of the U oxidation states.

Clearly the broadening and the shape of the L_3 -edge U(VI) NEXAFS peak follow from the ligand field and spin-orbit splitting of the 6d excited level. This relationship is examined further by considering variations in $d(\text{U-O})$ which should change the 6d ligand field splitting and, hence, the NEXAFS broadening. In Table I, we present properties of the 6d orbital and the NEXAFS full width at half-maximum, FWHM, for four different $d(\text{U-O})$. As well as $d(\text{U-O})=2.09\text{\AA}$ for $\delta\text{-UO}_3$, [15] shorter $d(\text{U-O})=2.04$ and 2.09\AA , which are found for other U(VI) minerals, [25] and a longer $d(\text{U-O}) = 2.15\text{\AA}$. The last distance tests the effect of an extreme change of $d(\text{U-O})$ for the U(VI) oxidation state. For $d(\text{U-O})=2.09\text{\AA}$, the t_{2g} spin-orbit splitting is 0.5 eV and the ligand field splitting from the lowest t_{2g} level to e_g is 6.7 eV, which is similar to the splitting of the intense NEXAFS peaks in Fig. 1(a). The dominantly 6d orbitals are anti-bonding combinations of U cation and O(2p) orbitals [11, 19] and the orientation of the e_g orbitals favors a stronger anti-bonding mixing with the O(2p) orbitals. [10, 11] The extent of the covalent mixing can be estimated from the $r_{\text{avg}}(t_{2g})$ and $r_{\text{avg}}(e_g)$ given in Table I, especially compared to the r_{avg} for the 6d orbitals of the isolated U^{6+} cation where $r_{\text{avg}}=1.7\text{\AA}$ for both the $6d_{3/2}$ and $6d_{5/2}$ orbitals. The UO_3 $r_{\text{avg}}(t_{2g})$, which is a weighted average of the sizes of the spin-orbit split t_{2g} components, is very close to the value for the isolated U cation showing that the t_{2g} covalent mixing is small. On the other hand, the 25 % increase of $r_{\text{avg}}(e_g)$ over $r_{\text{avg}}(t_{2g})$ is a clear indication of a substantial covalent mixing for the e_g orbitals. A strong anti-bonding character for the e_g orbital explains, in chemical terms, the large ligand field splitting and the consequent large FWHM of the U L_3 -edge NEXAFS. While the NEXAFS only directly reflects the covalent mixing in the ground state unoccupied 6d levels, there must be a comparable bonding covalent character in the filled dominantly O(2p) orbitals of the appropriate symmetry. [13] Indeed, this covalent character is found for the occupied orbitals of UO_x . [10-12] Thus the large FWHM of the U L_3 -edge NEXAFS edge is evidence for the covalent mixing and chemical interaction in the ground state of U(VI) in UO_3 . The t_{2g} spin-orbit splitting does not change significantly for the different $d(\text{U-O})$ in Table I, fully consistent with a minor involvement of the t_{2g} in the U-O chemical interaction leaving it a

dominantly atomic U(6d) orbital for all d(U-O). However, the ligand field splitting, $\Delta\epsilon(e_g)$, decreases monotonically with increasing d(U-O), fully consistent with a reduced covalent anti-bonding character between U(6d) and O(2p) as d(U-O) is increased. The reduced chemical interaction is also shown by the monotonic decrease in $r_{\text{avg}}(e_g)$ with increasing d(U-O). These changes in the U-O interaction explain why the NEXAFS FWHM also decreases monotonically with increasing d(U-O). As we show below, the direct connection between d(U-O) and the NEXAFS FWHM explains the changes in the L_3 -edge NEXAFS for different oxidation states of U. Another NEXAFS feature which reflects the changing chemical interaction for different d(U-O) is the branching ratio between the t_{2g} and e_g peaks. In Fig. 2, our theoretical NEXAFS for the three d(U-O) consistent with U(VI) oxides are superimposed. As expected from the data in Table I, the three spectra are quite similar to each other. The shapes of the peaks show that the branching ratio between the final states of e_g and t_{2g} character changes monotonically with d(U-O). The relative intensity of the e_g final states is smallest at d(U-O)=2.04Å and largest at d(U-O)=2.09Å where the top of the broadened peak becomes more nearly flat.

For U(V), the determinants for the NEXAFS final states have 3 electrons in the 2p shell, one electron in the "5f" spinors and one electron in an excited orbital. The angular momentum coupling of these open shells gives rise to a large number of determinants. It is clear from Fig. 1(b) that many terms, not just 3 as for U(VI), contribute to the U(V) NEXAFS; see the ESI for further discussion. However, it is possible to associate the features that have the highest intensity, with excited states separated by ligand field splitting of t_{2g} and e_g orbitals. States from over 30 terms around $E_{\text{rel}} \approx 3$ eV and $E_{\text{rel}} \approx 8.5$ eV make large contributions to the intensity in these energy regions with states of largely e_g character contributing to the higher E_{rel} peaks and states of t_{2g} character contributing to the lower E_{rel} peaks. The branching ratio for e_g and t_{2g} excitations leads to the relatively flat top at the maximum of the NEXAFS. In the ESI we show that the U(V) L_3 -edge NEXAFS for two other d(U-O) are similar to that in Fig. 1(b).

While for U(IV), with two electrons in the "5f" open shell, the number of states in the CI is dramatically increased, our open shell CI can adequately describe this case; see the ESI. From Fig. 1(c), it is clear that there are still two dominant groups of contributions to the NEXAFS at $E_{\text{rel}} \approx 3$ eV and $E_{\text{rel}} \approx 10$

eV with the lower and higher E_{rel} groups arising dominantly from configurations with excitations into t_{2g} and into e_g , respectively. The branching ratio for U(IV) yields a strongly asymmetric NEXAFS peak. This asymmetry coupled with a reduction in the ligand field splitting contribute to reducing the NEXAFS FWHM from 14.1 eV for U(V) to 13.25 eV for U(IV). Our results are consistent with the narrowing of the L_3 -edge NEXAFS observed for U(IV) in BaUO_3 [4] although not quite to the extent reported. To more completely test our model for U(IV), we have determined the NEXAFS for U(IV) in UO_2 ; see below.

A direct comparison of our predictions for the L_3 -edge NEXAFS for different oxidation states is presented in Fig. 3 with superposed spectra for octahedral U(VI), U(V), and U(IV) as well as for U(IV) in UO_2 . We compare our theoretical results with experiment around the NEXAFS maximum since this region is determined by the discrete excitations that we have considered; see the ESI. Importantly, the FWHM for U(V) is smaller than for U(VI); this holds as well for the other d(U-O) considered in Fig. 2 and in the ESI. In addition, the peak tops for U(V) are narrower than for U(VI). This is consistent with experimental data [4-6] and is a novel new way of distinguishing these oxidation states. Furthermore, our predictions for a narrow and symmetric NEXAFS peak for UO_2 are mirrored in the UO_2 peak in Fig. 4 of Ref. [6] In the fluorite structure neither the $6d(t_{2g})$ or the $6d(e_g)$ is directed toward the O ligands and this may contribute to a reduced t_{2g} - e_g splitting for U(IV) in fluorite UO_2 , which, in turn, reduces the FWHM of the NEXAFS peaks.

Our theoretical analysis of the U L_3 -edge NEXAFS is based on excitations to ligand field and multiplet split covalent discrete levels where the angular momentum coupling of the core and valence open shells is accurately treated. The good agreement of our predictions with experiment gives strong confidence in our theoretical approach. We have reproduced the main features of the observed NEXAFS for the different oxidation states and proven that the shape of the L_3 edge directly reflects the U oxidation state. This shape and the broadening of the edge arise mainly from the ligand field splitting of the unoccupied U(6d) level, which, in turn is related to the covalent mixing of the cation and anion orbitals. This work explains the chemical and physical origins of the broadening and shape of the L_3 -edge

NEXAFS and lays the foundation for using NEXAFS, together with rigorous theory, to obtain information about the geometric structure and the chemical interactions in heavy metal ionic compounds.

We acknowledge support by the Geosciences Research Program, Office of Basic Energy Sciences, U.S. DOE.

Table I. Properties of the 6d orbitals for UO_6 cluster models of U(VI) for different $d(\text{U-O})$, in Å. The relative orbital energies, $\Delta\varepsilon$ in eV, are given with the energy of the lowest spin-orbit split t_{2g} orbital set at $\Delta\varepsilon=0$; the spin orbit split $\varepsilon(t_{2g})$ are shown in parenthesis. The sizes of the orbitals, r_{avg} in Å, and the FWHM, in eV, of the U L_3 -edge NEXAFS are also given. See text for additional details.

$d(\text{U-O})$	$\Delta\varepsilon(t_{2g})$	$r_{\text{avg}}(t_{2g})$	$\Delta\varepsilon(e_g)$	$r_{\text{avg}}(e_g)$	FWHM
2.04	(0,0.5)	1.7	7.1	2.2	14.7
2.07	(0,0.5)	1.7	6.8	2.1	14.6
2/09	(0,0.5)	1.7	6.7	2.1	14.4
2.15	(0,0.5)	1.7	6.2	2.0	13.7

*bagus@unt.edu

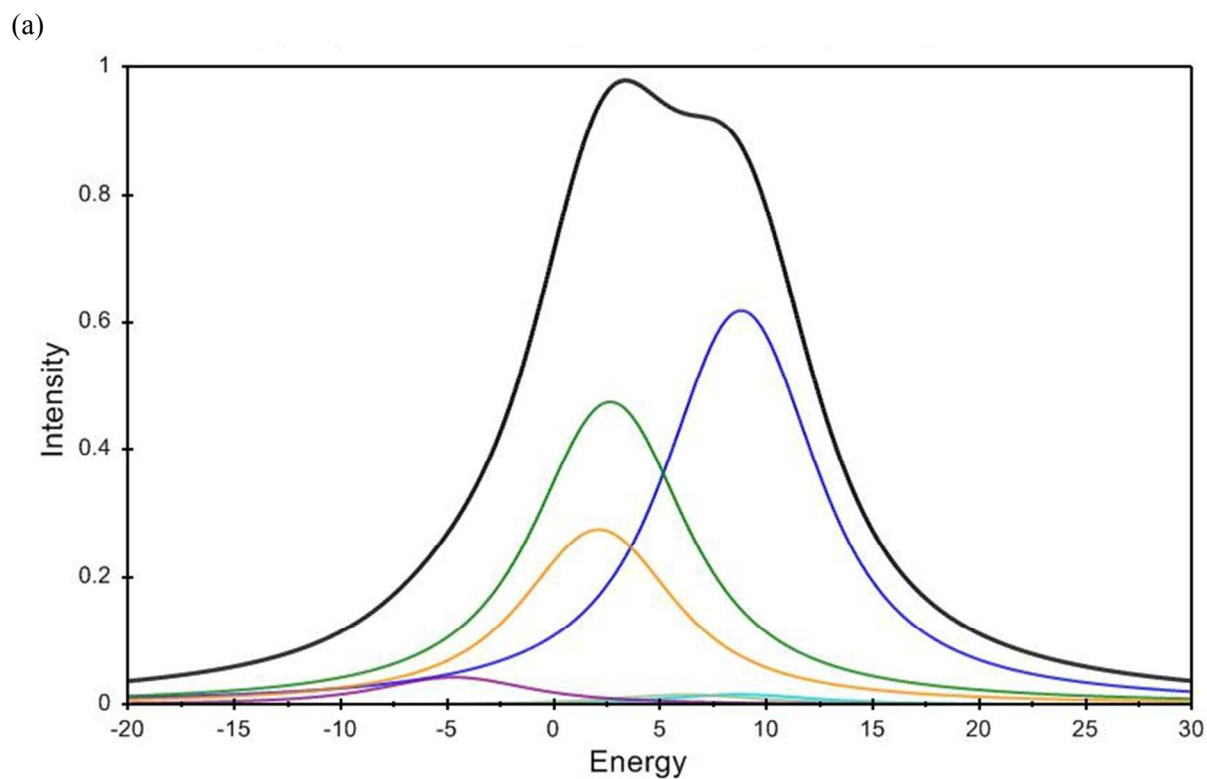
Figure Captions

Figure 1. Theoretical L_3 -edge NEXAFS spectra for UO_6 cluster models of (a) U(VI) with $d(\text{U-O}) = 2.09$ Å, (b) U(V) with $d(\text{U-O}) = 2.15$ Å, and (c) U(IV) with $d(\text{U-O}) = 2.22$ Å. The relative energies of each spectra are chosen so that $E_{\text{rel}}=0$ is at the inflection point of the leading edge of the spectra and the theoretical intensities are broadened with a Voigt convolution.

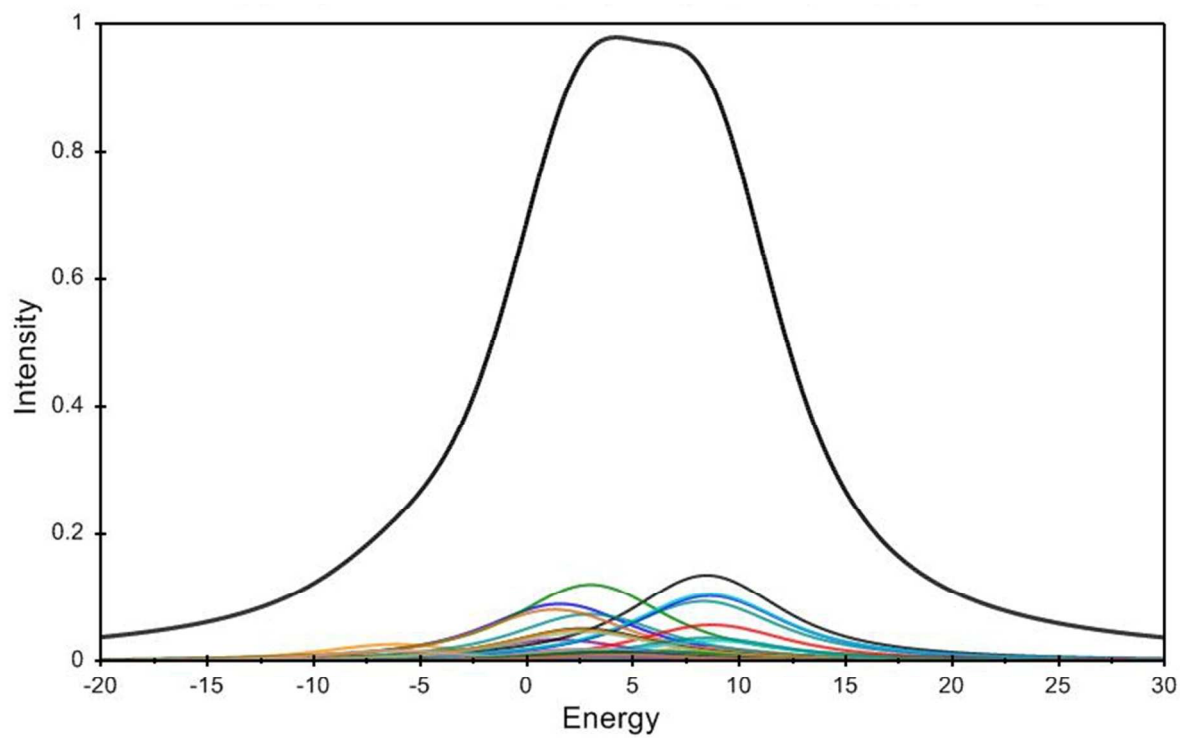
Figure 2. Comparison of theoretical L_3 -edge NEXAFS spectra for octahedral U(VI) for $d(\text{U-O})=2.04$, 2.07, and 2.09Å. The spectra are aligned and Voigt broadened as in Fig. 1.

Figure 3. Comparison of theoretical L_3 -edge NEXAFS for octahedral U(VI), U(V), and U(IV) and for U(IV) in fluorite UO_2 . The spectra for the different clusters are aligned with their inflection points at $E_{\text{rel}}=0$. The I_{rel} are broadened as in Fig. 1.

Figure 1. Theoretical L_3 -edge NEXAFS spectra for UO_6 cluster models of (a) U(VI) with $d(U-O) = 2.09$ Å, (b) U(V) with $d(U-O) = 2.15$ Å, and (c) U(IV) with $d(U-O) = 2.22$ Å. The relative energies of each spectra are chosen so that $E_{rel}=0$ is at the inflection point of the leading edge of the spectra and the theoretical intensities are broadened with a Voigt convolution.



(b)



(c)

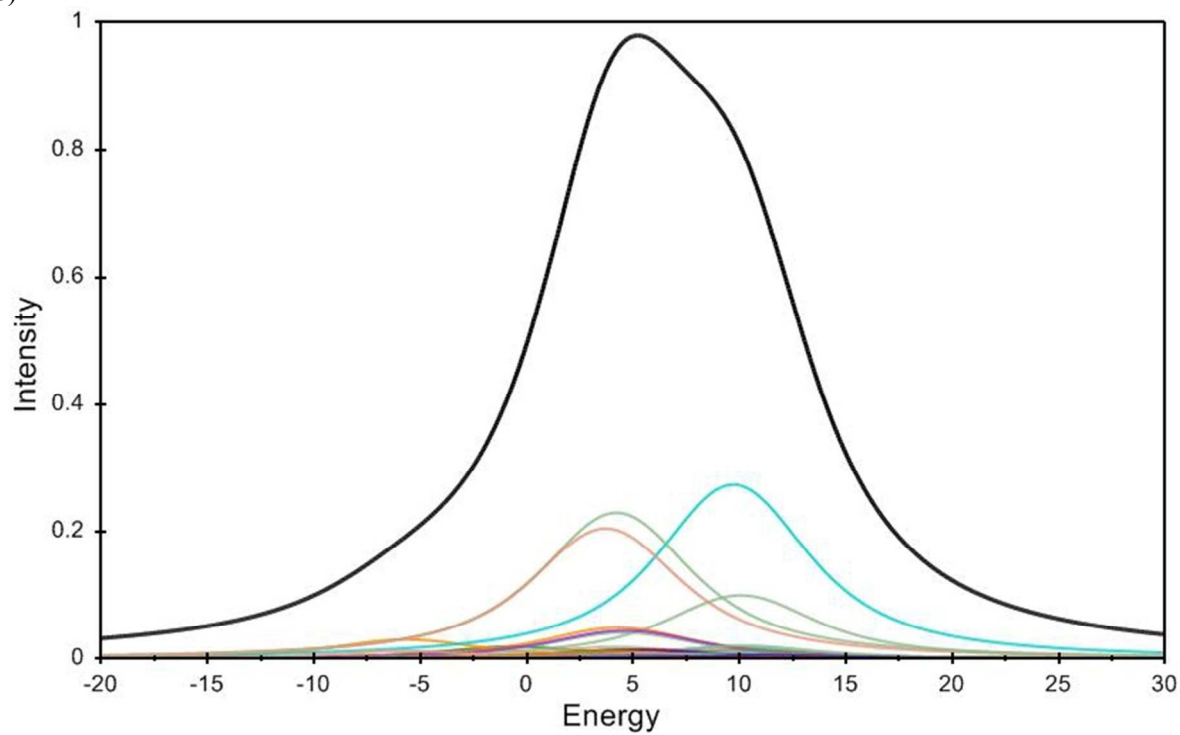


Figure 2. Comparison of theoretical L_3 -edge NEXAFS spectra for octahedral U(VI) for $d(\text{U-O})=2.04$, 2.07, and 2.09 Å. The spectra are aligned and Voigt broadened as in Fig. 1.

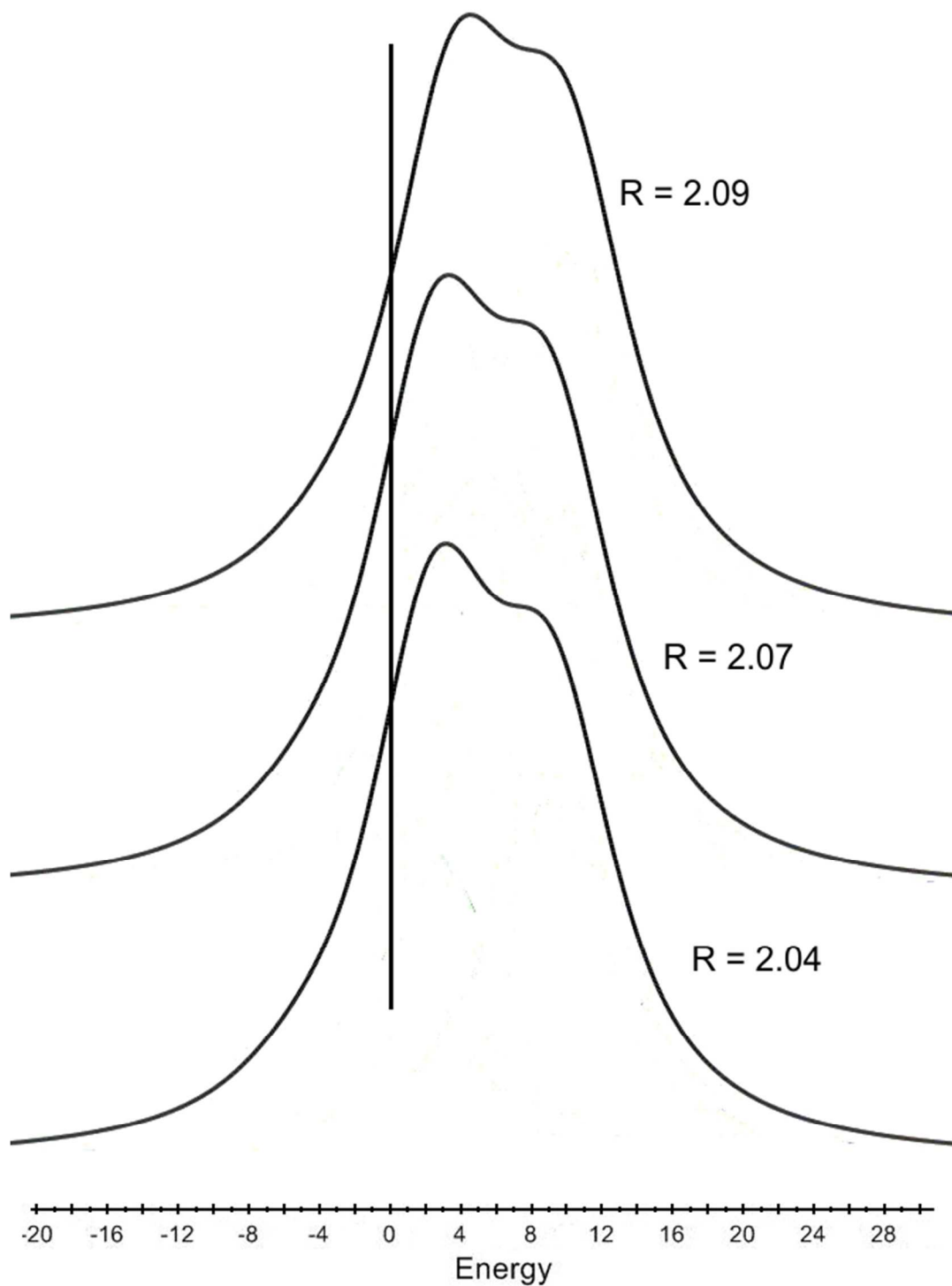
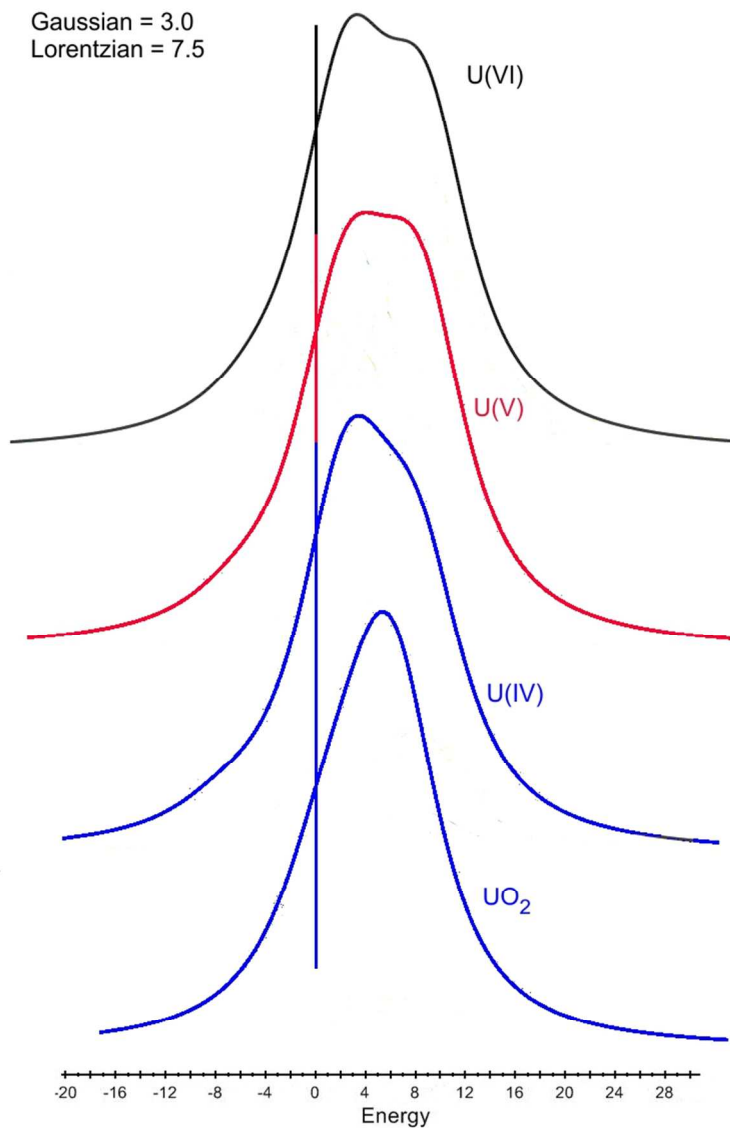


Figure 3. Comparison of theoretical L_3 -edge NEXAFS for octahedral U(VI), U(V), and U(IV) and for U(IV) in fluorite UO_2 . The spectra for the different clusters are aligned with their inflection points at $E_{rel}=0$. The I_{rel} are broadened as in Fig. 1.

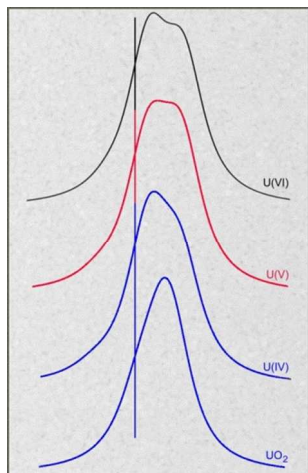


1. J. Stöhr, *NEXAFS Spectroscopy* (Springer-Verlag, Berlin, 1992).
2. G. Kalkowski, G. Kaindl, W. D. Brewer, and W. Krone, *Phys. Rev. B* **35**, 2667 (1987).
3. S. W. Yu, J. G. Tobin, J. C. Crowhurst, S. Sharma, J. K. Dewhurst, P. Olalde-Velasco, W. L. Yang, and W. J. Siekhaus, *Phys. Rev. B* **83**, 165102 (2011).

4. A. V. Soldatov, D. Lamoen, M. J. Konstantinovic, S. Van den Berghe, A. C. Scheinost, and M. Verwerft, *J. Solid State Chem.* **180**, 54 (2007).
5. S. Van den Berghe, M. Verwerft, J. P. Laval, B. Gaudreau, P. G. Allen, and A. Van Wyngarden, *J. Solid State Chem.* **166**, 320 (2002).
6. E. S. Ilton, J. S. L. Pacheco, J. R. Bargar, Z. Shi, J. Liu, L. Kovarik, M. H. Engelhard, and A. R. Felmy, *Environmental Science & Technology* **46**, 9428 (2012).
7. A. Kotani, H. Ogasawara, and T. Yamazaki, in *Physical properties of actinide and rare earth compounds. Search for heavy fermion characters* (Japanese Journal of Appl. Phys, 1993), p. 117.
8. A. Kotani and H. Ogasawara, *Physica B* **186-188**, 16 (1993).
9. A. Kotani and T. Yamazaki, *Progress of Theoretical Physics Supplement*, 117 (1992).
10. P. S. Bagus, E. S. Ilton, and C. J. Nelin, *Surf. Sci. Rep.* **68**, 273 (2013).
11. P. S. Bagus and C. J. Nelin, *J. Electron Spectrosc. Relat. Phenom.*, in press (2014).
12. P. Bagus, C. Nelin, and E. S. Ilton, *J. Chem. Phys.* (in press).
13. P. S. Bagus and E. S. Ilton, *Phys. Rev. B* **73**, 155110 (2006).
14. J. J. Rehr and A. L. Ankudinov, *Coord. Chem. Rev.* **249**, 131 (2005).
15. M. T. Weller, P. G. Dickens, and D. J. Penny, *Polyhedron* **7**, 243 (1988).
16. E. S. Ilton and P. S. Bagus, *Surf. Interface Anal.* **43**, 1549 (2011).
17. E. S. Ilton and P. S. Bagus, *Surf. Sci.* **602**, 1114 (2008).
18. L. Visscher, O. Visser, P. J. C. Aerts, H. Merenga, and W. C. Nieuwpoort, *Comput. Phys. Commun.* **81**, 120 (1994).
19. P. S. Bagus, E. S. Ilton, R. L. Martin, H. J. A. Jensen, and S. Knecht, *Chem. Phys. Lett.* **546**, 58 (2012).
20. F. Zhou and V. Ozolins, *Phys. Rev. B* **83**, 085106 (2011).
21. G. Burns, *Introduction to Group Theory With Applications* (Academic Press, New York, 1977).
22. M. O. Krause and J. H. Oliver, *J. Phys. Chem. Ref. Data* **8**, 329 (1979).

23. G. van der Laan, K. T. Moore, J. G. Tobin, B. W. Chung, M. A. Wall, and A. J. Schwartz, *Phys. Rev. Lett.* **93**, 097401 (2004).
24. P. S. Bagus, H. Freund, H. Kühlenbeck, and E. S. Ilton, *Chem. Phys. Lett.* **455**, 331 (2008).
25. P. C. Burns, *Canadian Mineralogist* **43**, 1839 (2005).

Table of Contents
Theoretical Analysis of the U L₃-Edge NEXAFS in U Oxides
Connie J. Nelin, Paul S. Bagus^{*} and Eugene S. Ilton



Text: Rigorous theoretical studies establish the importance of ligand field and multiplet splitting for the L₃-edge NEXAFS of U oxides,